Journal of Electronic Materials (2021) 50:6607–6614
https://doi.org/10.1007/s11664-021-09255-2

ELECTRONIC PACKAGING AND INTERCONNECTIONS 2021

Check for updates

Microstructural Coarsening and Mechanical Properties of Eutectic Sn-58Bi Solder Joint During Aging

Fengjiang Wang[1,2] · **Amey Luktuke**[1] · **Nikhilesh Chawla**[1]

Received: 25 June 2021 / Accepted: 22 September 2021 / Published online: 7 October 2021

Abstract

With miniaturization and heterogeneous integration in packaging, there has been a drive toward developing lower temperature solders. Sn-58Bi eutectic solder provides an attractive alternative with its meting point at 138°C. Due to the lower melting temperature of Sn-Bi solder, Bi coarsening may occur even at room temperature. In this paper, the microstructural evolution in Sn-58Bi joints was observed during room temperature storage. Room temperature aging induced the dissolution and coarsening of Bi phases in the solder matrix, especially in the primary Sn phases and Sn-Bi dendrites. The mechanical properties of individual Sn-rich and Bi-rich phases were measured by nanoindentation. The results showed that the Sn-rich phases had higher Young's modulus and hardness than Bi-rich phases in aged solder joints due to solution strengthening. Bi phases were more compliant and had lower hardness than Sn.

Keywords Sn-Bi solder · phase size distribution · aging · phase coarsening · nanoindentation

Introduction

For many years, Pb-Sn eutectic solder had been widely used as the interconnect material of choice in the electronics industry. Due to the harmful effects of lead on the human body and the environment, the development of Pb-free solders has been driven by the European Union's Restriction of Hazardous Substances Directive (RoHS) and Waste from Electrical and Electronic Equipment (WEEE) legislation.[1] Among all the developed alloy systems, Sn-Ag-Cu solder has been used extensively due to its superior combination of wettability, reliability, and mechanical properties.[2,3] However, with thinner flip-chip as well as heterogeneous integration in packaging emerging, the higher melting point of Sn-Ag-Cu solder will induce larger warpage of the components during reflow, as well as damage to other lower point materials (e.g., polymers). Thus, there is a driving force to developing solders with lower melting temperature.

✉ Nikhilesh Chawla
nikc@purdue.edu

1 School of Materials Engineering, Purdue University, West Lafayette, IN 47906, USA

2 School of Materials Science and Engineering, Jiangsu University of Science and Technology, Zhenjiang 212003, China

The Sn-Bi solder system is a promising Pb-free solder with a relatively low melting point.[4,5] From the Sn-Bi binary phase diagram,[6] as shown in Fig. 1, there exists a eutectic reaction with the composition of Sn-58Bi at a temperature of 138°C. Moreover, there also exists a solid solution for Bi atoms in β-Sn phase with a composition ranging from 0 wt.% to 21 wt.%. Thus, many studies have been carried out with relatively small additions of Bi to Sn-Ag-Cu solder to take advantage of the solution strengthening. For example, Ei-Daly et al.[7,8] added small amounts of Bi into Sn-1.5Ag-0.7Cu solder and found that 1.0 wt.% Bi addition significantly enhanced the solid solution effect of Bi, refined the intermetallic compound (IMC) particles, and increased the mechanical strength and Young's modulus of the solder. He et al.[9] investigated the effect of Bi addition on the creep properties of Sn-3.0Ag-0.5Cu solder, and also verified that Bi addition improved the creep resistance of the solder at higher temperatures. Celikin et al.[10] further investigated the creep properties with different Bi addition into Sn-0.6Ag-0.7Cu solder, and found that the creep resistance deteriorated with an increase of Bi addition. Liu et al.[11] provided a systematic review on strengthening methods, strengthening mechanisms and the effect on strain rate sensitivities of lead-free solders with Bi addition. Belyakov et al.[12] investigated the precipitation and coarsening kinetics of Bi plates in Sn-Ag-Cu-Bi and Sn-Cu-Ni-Bi solders during room temperature storage, and obtained the probable orientation relationships between Bi and β-Sn for the precipitation of Bi plates.

Depending on the composition of the alloy, Bi may exist in solid solution with the β-Sn phase or precipitate from β-Sn phases. Shang et al.[13] found that Bi atoms were easily passed through Cu-Sn IMCs and precipitated at the interface between IMC/Cu in Sn-58Bi solder joints during isothermal aging. A similar phenomenon was also found by Liu et al.[14,15] Kang et al.[16] investigated Bi precipitation on IMC growth in Sn-58Bi/Cu joints during isothermal aging, and found that the growth of Cu_6Sn_5 at the interface was promoted by Bi precipitation. It can be found that most of the studies on Bi precipitation or segregation have been carried out on the solder/IMC interface.

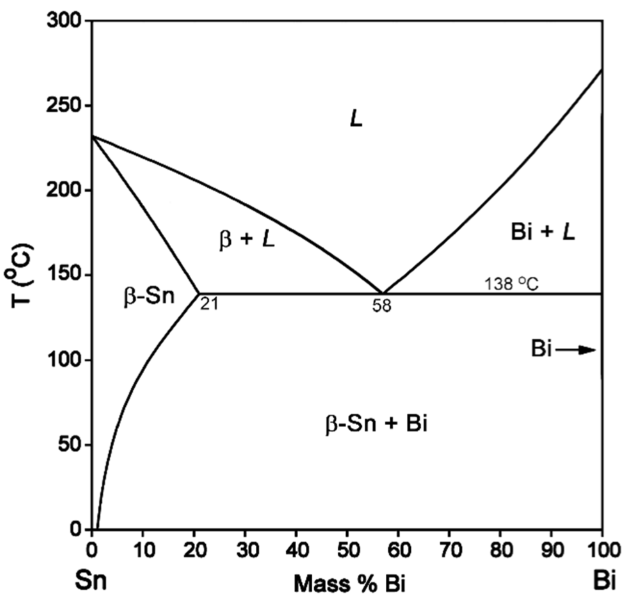

Fig. 1 Sn-Bi binary phase diagram[6].

In general, there is very limited data on Bi redistribution and microstructural coarsening during annealing of Sn-Bi solder joints, particularly away from the solder/IMC interface. In this work, we provide an understanding of microstructural evolution (coarsening) in Sn-58Bi solder joints during room temperature aging. We also conducted nanoindentation studies on the individual phases formed in the Sn-58Bi solder. We show that the Bi phase is not quite "brittle" as previously reported.

Materials and Experimental Procedure

Sandwich solder samples, with copper on either side and Sn-58Bi in the middle, were used in this study. Sn-58Bi foil with a thickness of 300 μm was sandwiched between Cu discs with diameter of 0.95 cm and thickness of 0.5 cm. The Cu discs were ground and polished to a 0.05 μm final finish with colloidal silica suspension. Solder foil was cut into pieces with a diameter of 0.95 cm. Before soldering, the Cu discs and solder foil were cleaned with acetone. Figure 2 shows the preparation of the Sn-58Bi solder joints including the assembly and reflowing parameters. A thin foil of solder was placed in between the two Cu discs coated with Indalloy Flux #5 RMA (Rosin Mildly Activated, Temperature Range: 125–350°C) (Indium Corporation), as shown in Fig. 2a. The temperature was measured using a thermocouple touching the bottom Cu disc of the sandwich solder joint. The joints were reflowed at a peak temperature of 170°C, and then rapidly cooled at a rate of 4°C/s on a large Cu block that served as a heat sink. The soldered joints were then aged at room temperature (25°C) for various times. The as-soldered and aged joints were cross-sectioned, mounted in epoxy and also

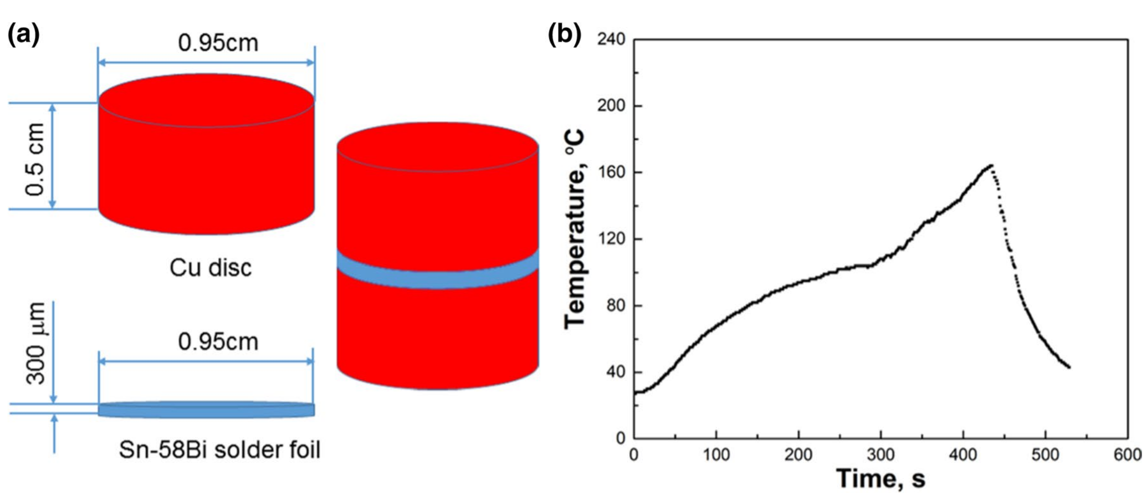

Fig. 2 Preparation on solder joints: (a) assembling of joint and (b) reflowing parameter.

polished to a 0.05 μm final finish with colloidal silica suspension. The microstructural evolution in the solder joints was quantified by studying the microstructure, at different aging time steps, by scanning electron microscopy (SEM). Energy dispersive spectroscopy (EDS) was also carried out to determine the mapping at selected areas.

Results and Discussion

We begin by describing the microstructure of the starting microstructures of the Sn-58Bi/Cu joints. Figure 3 shows SEM images of the cross-sections of the solder joint. Sn-rich dendrites are observed surrounded by a lamellar eutectic of Sn-rich and Bi phases. Closer inspection of the eutectic shows some areas that are primarily Sn but with precipitated Bi particles. A very thin Cu_6Sn_5 layer was also formed at the solder/Cu interface.

Figure 4a shows a higher magnification image of the solder microstructure in as-soldered Sn-58Bi joint. The gray and white areas are Sn-rich and Bi-rich phases, respectively. Due to the rapid cooling from Cu heat sink, several regions of primary β-Sn phases were observed due to the non-equilibrium solidification. During the melting of Sn-58Bi solder, the solute content of Bi in β-Sn can reach a maximum of 21 wt.% Bi at 138°C, which gradually decreases with continuous cooling. Thus, precipitated Bi particles can be observed in the primary β-Sn phase in Fig. 4a.

Due to the relatively low melting point of Sn-58Bi solder, room temperature is a high fraction of the melting point, T_m. Thus, aging at room temperature can induce microstructural change in the solder matrix. Figure 4 shows the microstructural evolution of the Sn-58Bi solder matrix with different aging times at room temperature, ranging from 15 to 263 days. With increasing aging time, the size of Bi phases in the lamellar eutectic structure increased. The initially precipitated Bi particles also gradually dissolved into the primary β-Sn phases, especially after 263 days, as shown in Fig. 4d. With the coarsening of Bi phases and dissolution of Bi particles, the fraction of Bi phases decreased, as shown in Fig. 5. After soldering, the area fraction of Bi phases in the microstructure was 47%, but after 263 days aging, it decreased to about 44.6%. Therefore, the Bi coarsening and Bi dissolution took place during room temperature aging, even at short annealing times. After a longer aging period with 263 days, the primary β-Sn phases become more clear after dissolution of the Bi phase.

To further investigate the dissolution behavior of precipitated Bi particles into β-Sn phases, image analysis was used to measure the size distribution of Bi particles as a function of aging time, as shown in Fig. 6. The selected area, marked in Fig. 6a and b, was from the solder joints after soldering and aging for 45 days, respectively. Figure 6c shows the size distribution of Bi particles in these marked areas. Due to the oxidation on the sample with long-term aging, the surface was slightly polished, and accordingly, Bi particles in the same location was not observed for the sample after 263 days aging. In the as-soldered microstructure, most of the Bi particles are distributed within an area of less than 0.2 μm^2. With room temperature aging, the number of Bi particles clearly decreased while their area increased to about 0.5 μm^2. It was verified that the Bi particles were coarsened and dissolved into β-Sn phases during room temperature aging, which can be clearly observed by the elemental mapping shown in Fig. 7. According to phase diagram, the Bi solubility in the Sn matrix under equilibrium conditions is 1.75 wt%. However, from the quantitative EDS analysis of the Sn matrix after reflow, the Bi content is about 5.5 wt% Bi in the matrix, indicating some supersaturation due to the faster cooling rate (relative to equilibrium conditions).

To further investigate the room temperature aging on the phase coarsening, the size distributions of the individual Sn and Bi phases in the eutectic Sn-58Bi solder were determined by measuring the linear intercepts (a total of 400) on

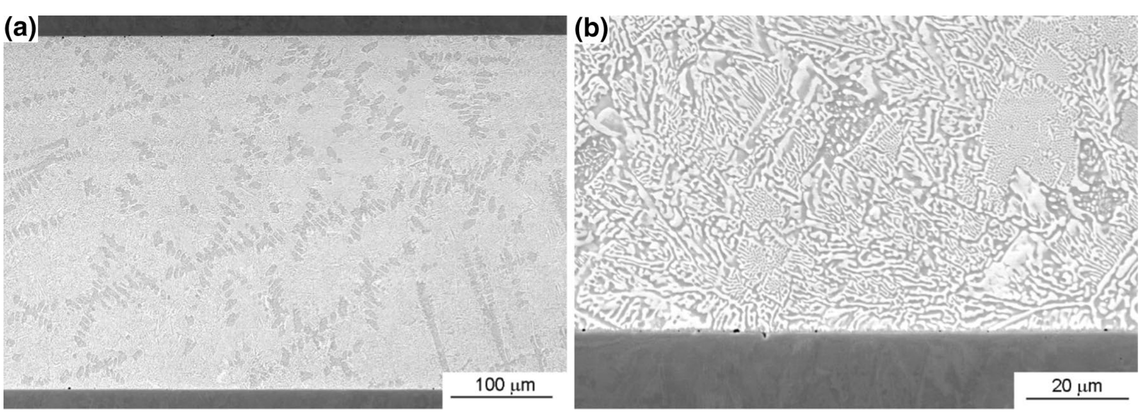

Fig. 3 SEM images of the cross-sectional microstructure in as-soldered Sn-58Bi joint with (a) whole solder joint and (b) interfacial structure.

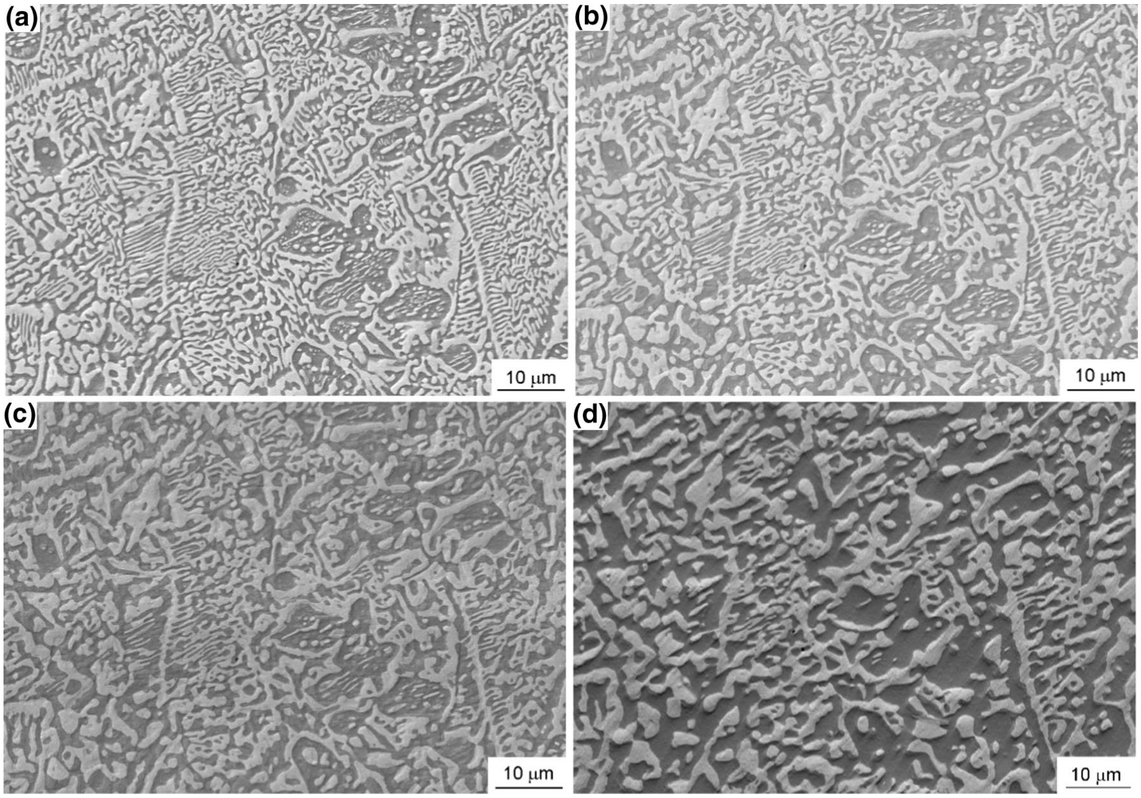

Fig. 4 SEM microstructures of the solder matrix in (a) the initial as-soldered joints and (b–d) after room temperature aging for 15 days, 45 days and 263 days, respectively.

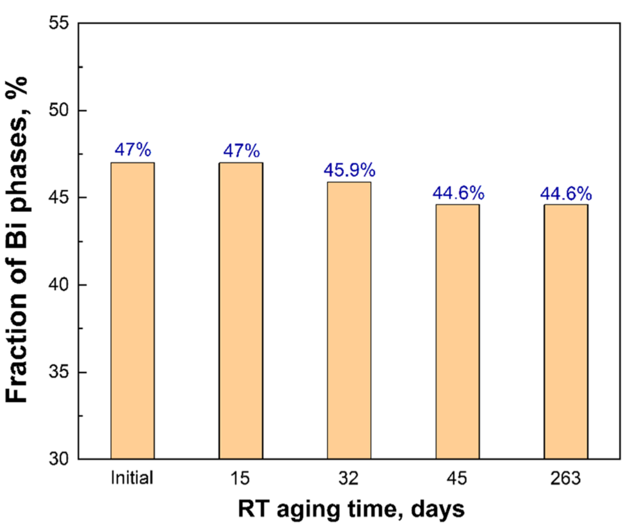

Fig. 5 Relationship between the fraction of Bi phases with storage times.

randomly drawn lines on the SEM microstructure in Fig. 4. The phase size distributions (PSDs) of the individual Sn and Bi phases for different storage times are presented in Fig. 8. It should be noted that the height of the peak decreases and the width of the PSD increases with room-temperature storage. Moreover, the PSD of Sn phases were similar to that of the Bi phases, which were not influenced by the storage time.

After aging, the mechanical properties of individual β-Sn and Bi phases were measured using nanoindentation. Continuous stiffness measurement with a maximum load at 1 mN was used with 10×10 arrays, as shown in Fig. 9. The distance between two adjacent indentations was set at 6 μm to make sure that the plastic zones around individual indentations did not overlap. From Fig. 9, the indents on individual β-Sn and Bi phases are marked with circles. Fig. 10 shows the relationship between Young's modulus and hardness and nanoindentation depth for the β-Sn and Bi phases. The Young's modulus was 48.4 ± 4.3 GPa and 34.3 ± 2.5 GPa, and hardness was 0.52 ± 0.05 GPa and 0.4 ± 0.05 GPa for the β-Sn and Bi phases, respectively. Most studies on investigating the mechanical behavior of Sn-58Bi solder primarily focus on studying the fracture surface. Liu et al.[17] reported the Bi segregation at the IMC-Cu interface upon thermal aging of Sn-58Bi solder. The reduction in fracture resistance of thermally-aged solder was attributed to the Bi segregation as Bi particles were observed on the fracture surface. Similarly, Mokhtari et al.[18] studied the fracture surface of as-reflowed Sn-58Bi

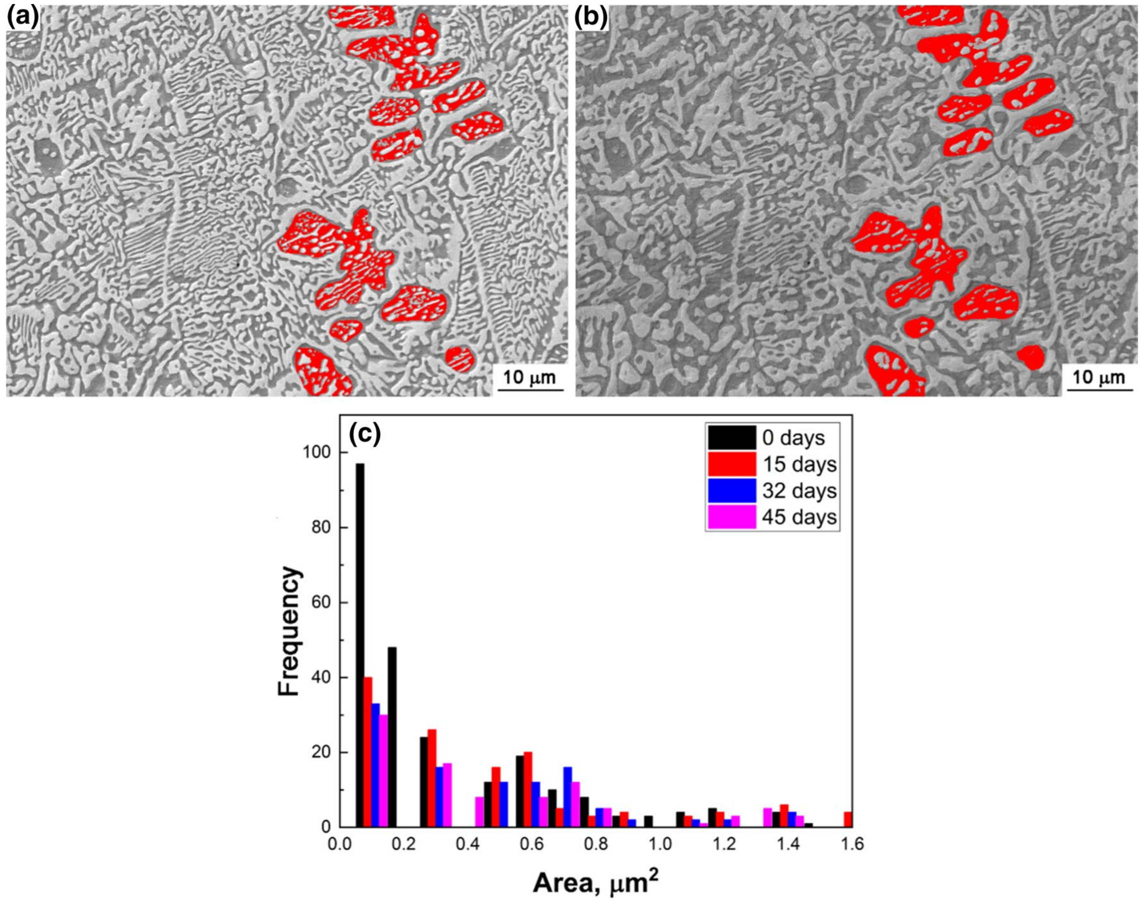

Fig. 6 (a–b) Distribution of precipitated Bi particles in the as-soldered joint and aged joint for 45 days, respectively. (c) Bi phase area size distribution in the marked areas.

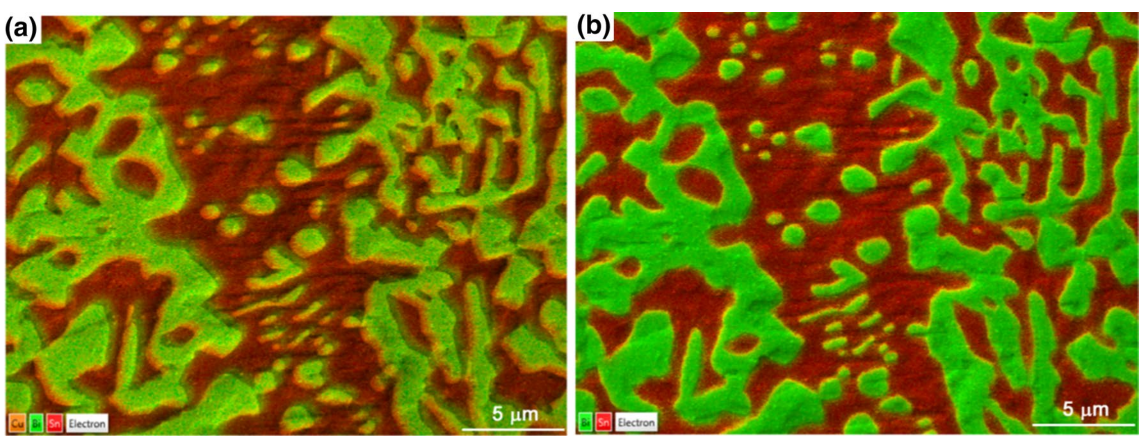

Fig. 7 Bi dissolution from elemental mapping in the aged joint after (a) 32 days and (b) 45 days, respectively.

solder after shear test, and found a brittle fracture surface with presence of coarsened Bi particles in it. The brittle nature of fracture surface is associated with the inherent brittleness of Bi phase. However, our results show that pure Bi is significantly softer than the Sn-solid solution phase, in terms of both stiffness and hardness. Yanaka et al.[19] studied the tensile stress-strain behavior of Bi single crystals and hypothesized that plastic deformation in

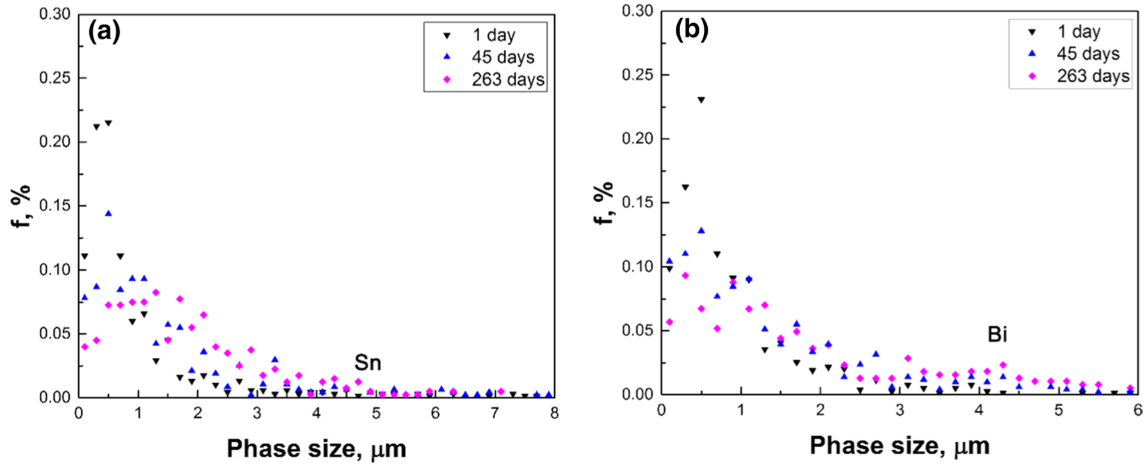

Fig. 8 Effect of storage times on the phase size distribution of (a) Sn phase and (b) Bi phase.

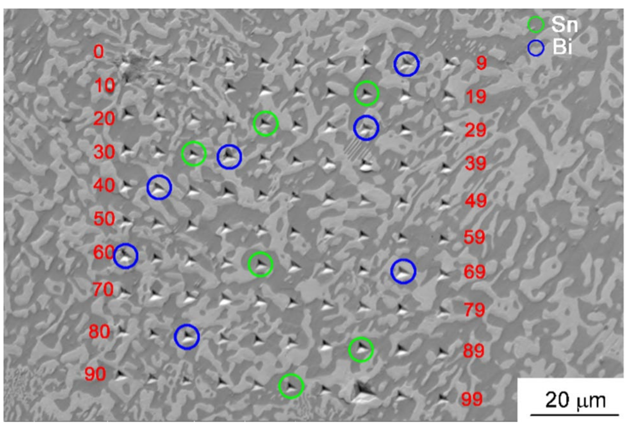

Fig. 9 Nanoindentation map on the solder matrix.

these materials occurs by twinning initially, followed by secondary slip. Thus, embrittlement due to Bi addition in solder needs to be investigated focusing on the cooperative deformation behavior between Bi and Sn phases.

Conclusions

In this paper we present the microstructural evolution in Sn-58Bi solder joints during the room temperature aging. The mechanical properties of individual β-Sn and Bi phases in Sn-58Bi solder joint was measured by nanoindentation. Our conclusions are as follows:

(1) The solder matrix in the Sn-58Bi solder joint was mainly composed of primary β-Sn phases with finely distributed precipitated Bi particles and a lamellar eutectic structure after soldering.
(2) During room temperature aging, Bi phases coarsened in the eutectic area, while the precipitated Bi particles gradually dissolved into the primary β-Sn phases.
(3) Nanoindentation illustrated that the Sn-rich phases had higher Young's modulus and hardness than Bi-rich phases in aged solder joints due to the solution strengthening. The pure Bi phase is more compliant and has lower hardness than β-Sn.

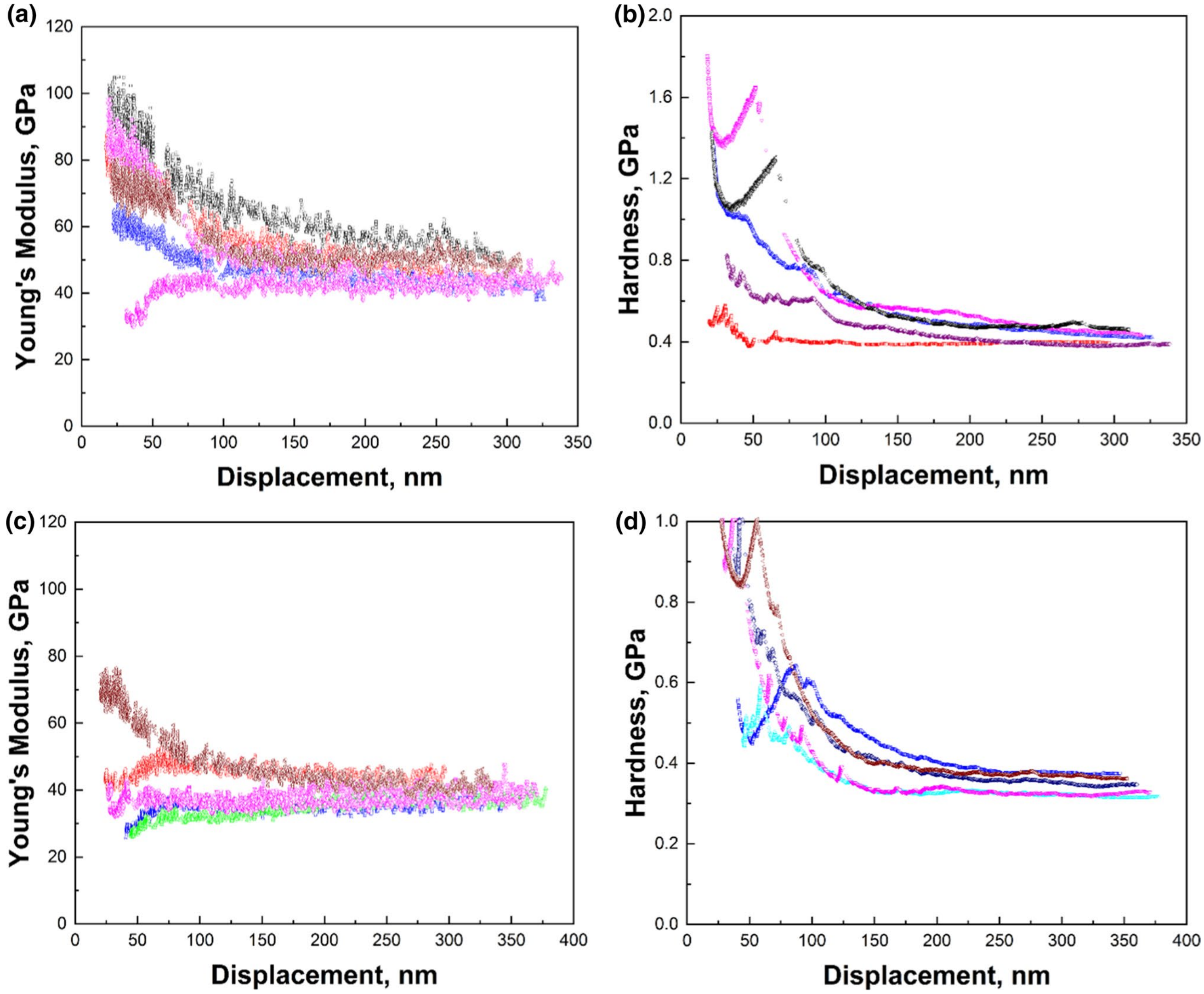

Fig. 10 Young's modulus and hardness of (a–b) β-Sn and (c–d) Bi-rich phases in the solder matrix.

Acknowledgments The authors gratefully acknowledge funding from the National Science Foundation (NSF), NSF-CMMI 1763128 (Program Manager: Dr. Alex Lewis). We also acknowledge start-up funds from Purdue University.

Conflict of interest The authors declare that they have no conflict of interest.

References

1. S. Cheng, C.-M. Huang, and M. Pecht, *A review of lead-free solders for electronic applications Micron. Reliab.* 75, 77 (2017).
2. L. Zhang, and K.N. Tu, *Structure and properties of lead-free solders bearing micro and nano particles Mater. Sci. Eng. R.* 82, 1 (2014).
3. D.A. Shnawah, M.F. Sabri, and I.A. Badruddin, *A review on thermal cycling and drop impact reliability of SAC solder joint in portable electronic products Microelectron. Reliab.* 52, 90 (2012).
4. F. Wang, H. Chen, Y. Huang, L. Liu, and Z. Zhang, *Recent progress on the development of Sn-Bi based low-temperature Pb-free solders J. Mater. Sci.-Mater. Electron.* 30, 3222 (2019).
5. H.R. Kotadia, P.D. Howes, and S.H. Mannan, *A review: on the development of low melting temperature Pb-free solders Micron. Reliab.* 54, 1253 (2014).
6. Binary Alloy Phase Diagrams, edited by T. Massalski (ASM, International, Materials Park, OH, 1986)
7. A.A. El-Daly, A.M. El-Taher, and S. Gouda, *Development of new multicomponent Sn-Ag-Cu-Bi lead-free solders for low-cost commercial electronic assembly J. Alloys Compd.* 627, 268 (2015).
8. A.A. El-Daly, A.M. El-Taher, and S. Gouda, *Novel Bi-containing Sn-1.5Ag-0.7Cu lead-free solder alloy with further enhanced thermal property and strength for mobile products Mater. Design.* 65, 796 (2015).
9. M. He, S.N. Ekpenuma, and V.L. Acoff, *Microstructure and creep deformation of Sn-Ag-Cu-Bi/Cu solder joints J. Electron. Mater.* 37, 300 (2008).
10. M. Celikin, M. Maalekian, and M. Pekguleryuz, *Effect of Bi additions on the creep behavior of SAC solder alloys J. Electron. Mater.* 47, 5842 (2018).

11. S. Liu, S. McDonald, K. Sweatman, and K. Nogita, *The effects of precipitation strengthening and solid solution strengthening on strain rate sensitivity of lead-free solders Microelectron. Reliab.* 84, 170 (2018).
12. S.A. Belyakov, J. Xian, G. Zeng et al., *Precipitation and coarsening of bismuth plates in Sn-Ag-Cu-Bi and Sn-Cu-Ni-Bi solder joints J. Mater. Sci.-Mater. Electron.* 30, 378 (2019).
13. P.J. Shang, Z.Q. Liu, D.X. Li, and J.K. Shang, *Directional growth of Cu3Sn at the reactive interface between eutectic SnBi solder and (100) single crystal Cu Scripta Mater.* 59, 317 (2008).
14. C.Z. Liu, and W. Zhang, *Bismuth redistribution induced by intermetallic compound growth in SnBi/Cu microelectronic interconnect J. Mater. Sci.* 44, 149 (2009).
15. F. Wang, H. Chen, Y. Huang, and C. Yan, *Interfacial behavior and joint strength of Sn-Bi solder with solid solution compositions J. Mater. Sci. Mater. Electron.* 29, 11409 (2018).
16. T.Y. Kang, Y.Y. Xiu, C.Z. Liu, L. Hui, J.J. Wang, and W.P. Tong, *Bismuth segregation enhances intermetallic compound growth in SnBi/Cu microelectronic interconnect J. Alloys. Compd.* 509, 1785 (2011).
17. P.L. Liu, and J.K. Shang, *Interfacial embrittlement by bismuth segregation in copper/tin-bismuth Pb-free solder interconnect J. Mater. Res.* 16, 1651 (2001).
18. O. Mokhtari, and H. Nishikawa, *Correlation between microstructure and mechanical properties of Sn-Bi-X solders Mater. Sci. Eng. A*. 651, 831 (2016).
19. Y. Yanaka, Y. Kariya, H. Watanabe, H. Hokazono, Plastic deformation behavior and mechanism of bismuth single crystals in principal axes. Mater. Trans. MD201503 (2016)